12-2021

Silver Microparticle and Submicron Wire - Polylactic Acid Composites for Additive Manufacturing

Jenna W. Robichaux
University of New Orleans, New Orleans, jswalke5@uno.edu

Silver Microparticle and Submicron Wire - Polylactic Acid Composites for Additive Manufacturing

A Thesis

Submitted to the Graduate Faculty of the
University of New Orleans
in partial fulfillment of the
requirements for the degree of

Master of Science
in
Engineering
Mechanical

by

Jenna Walker Robichaux

B.S. Louisiana State University, 2017

December, 2021

Acknowledgements

The most important acknowledgement of gratitude I wish to express is to my advisor, Dr. Damon A. Smith, for his guidance and patience during my graduate study. It has been an honor to be his graduate student and be guided during my graduate study in the Mechanical Engineering Department of the University of New Orleans. He has supported me throughout my research assistantship two years and academically through the rough road to finish this thesis as well.

I would also like to thank Dr. Paul J. Schilling and Dr. Paul D. Herrington for serving on my thesis committee. I am grateful to the department of Mechanical Engineering, the Advanced Materials Research Institute, and the Graduate School at the University of New Orleans.

I am indebted to Dr. Wendy Schluchter from the Biological Sciences Department at University of New Orleans and Dr. Jibao He from Tulane University for use of their laboratory facilities for the completion of this thesis.

I owe the sincerest of thanks to John Arnold, Cythniya Shrestha, Michael Wong, Alexis Blanco, Lyndsay Ann Carrigee, Kes Lynn Joseph, Mark Granier, Malachi Ophus, and Anthony Pela for their helping hands throughout this thesis.

I would like to recognize my friends, Daniel Harrell, Carl Hendrickson, Denis Pansolin, Zachary Schexnaydre, and Shivank Srivastava, at the University of New Orleans for their support and motivation.

Last but not the least, I will forever be thankful to my husband, Cameron Robichaux for his love, support, and encouragement to further my education. This thesis would not have been possible if it was not for his encouragement and inspiration and I would not be where I am today without his continued support of my dreams and aspirations.

This work was supported through funding from the University of New Orleans Office of Research Stimulating Competitive Research (SCoRe) program and the Louisiana Board of Regents Research Competitiveness Subprogram (RCS).

Table of Contents

List of Figures

List of Tables

Abstract

This thesis explores the incorporation of silver microparticle and submicron wire additives into thermoplastic filament feedstock for fused filament fabrication (FFF) to create multifunctional three-dimensional (3D) printable composites. The impact of silver microparticle and submicron wire additives on mechanical behavior along with antibacterial effect of the silver microparticle and submicron wire additives on printed objects were assessed.

Composite FFF filaments were fabricated by solution processing, granulation, and extrusion. Differential Scanning Calorimetry (DSC) was conducted to measure the glass transition and melting point temperatures of the composite filaments for 3D printing. The effect of the additive addition on the thermal properties and tensile mechanical performance was measured. Scanning Electron Microscopy (SEM) was used to analyze the composite microstructure and fracture behavior. The reduction in the growth of *Escherichia coli* (*E. coli*) was measured after exposure to FFF-printed composite test specimens with additive concentrations ranging from 0.0 to 10.0 weight percent.

Keywords: 3D Printing, Thermoplastic Composites, Fused Filament Fabrication, Mechanical Properties, Antibacterial Properties

I. Introduction

The geometric complexity and rapid customization achievable with additive manufacturing (AM) has created a great deal of interest in the field of biomedicine [Society of Manufacturing Engineers (SME) Annual Report, 2018; Jin et al., 2015]. Prosthetics, orthotics, splints, catheters, implants and specialty surgical tools are just a few of the numerous applications being pursued using AM technologies as a new approach to customized healthcare [Jin et al., 2015; Malik et al., 2015]. In many of these applications, it is important that the device be manufactured from a biocompatible material that is not prone to causing infections. Antibacterial materials are one of the several approaches the United States health care industry is currently using to reduce the approximately 1.7 million hospital-acquired infections (HAIs) that patients experience annually [Center for Disease Control and Prevention, 2017; Cloutier et al., 2015]. These infections are often acquired by exposure to bacteria present on equipment and instruments [Page et al., 2009]. Therefore, there is a significant need for AM materials in emerging biomedical applications to possess both biocompatibility and antibacterial properties.

Though several AM technologies are used for biomedical applications, fused filament fabrication (FFF) is the most popular process used because of the widespread availability of low-cost and reliable printing systems [Gibson et al., 2015]. Commercial FFF systems typically construct parts from a 1.75-or 3-mm diameter filament of a thermoplastic material that is fed by a stepper motor to an extruder head heated above the glass transition or melting temperature, for amorphous or semi-crystalline materials, respectively. The viscous filament material is deposited one layer at a time on to a stage to build up the desired three-dimensional (3D) design. Commercially available biocompatible filament options for FFF printers with antibacterial

properties are currently limited and relatively few studies exist in the scientific literature on these materials.

One common approach to impart antibacterial properties to polymeric materials is through the incorporation of antibacterial metals. Silver, in particular, has been widely used for centuries for its antimicrobial properties. The metal releases silver ions, which have a strong cytotoxic effect on fungi, protozoa, several viruses and both gram-positive and gram-negative bacteria [LeOuay and Stellacci, 2015; Palza et al., 2015; Chernousova and Epple, 2015]. Herein, the use of silver particles as an antibacterial additive in polylactic acid (PLA) filaments for use with commercial FFF systems is investigated. PLA is the most common thermoplastic material used for biomedical applications because of its biocompatibility, biodegradability, mechanical properties and its ease of processing [Saini et al., 2016]. A wide variety of micro- and nanoscale additives have been previously explored as a means of modifying the properties of, or adding additional functionality to, thermoplastics [Palza et al., 2015; Saini et al. ,2016; Blattmann et al., 2016; Doganay et al., 2016]. The use of silver microparticles and high aspect ratio wires with diameters in the intermediate submicron range are examined. While nanoparticle additives may exhibit novel properties attributed to their nanoscale dimensions or large surface-to-volume ratio, challenges related to processability and toxicity may exist in some materials systems [Blattmann et al., 2016; Hussain et al., 2009; Müller et al., 2017]. Therefore, this thesis examines the use of micron and submicron additives in an effort to reduce these challenges while still maintaining favorable surface interactions with the polymer matrix. The use of these additives for FFF printing of antibacterial objects is assessed and the impact on the mechanical behavior of the material is investigated.

II. Background

Additive manufacturing (as known as 3D printing) holds strong potential for the development and creation of a new class of multifunctional composites. Referred to in short as AM, the rudimentary principle of this technology is that a model, initially generated using a three-dimensional Computer-Aided Design (3D CAD) system, can be fabricated directly without the need for process planning.

AM works by adding material in layers with each layer being a thin cross-section of the part derived from the original CAD data. The thinner each layer is, the closer the final part is to the original. All commercialized AM machines use a layer-based approach. The major ways that they differ are in the materials that can be used, how the layers are created, and how the layers are bonded to each other.

Fused filament fabrication (FFF) is an additive manufacturing process. FFF is the most widely used 3D printing technology representing the largest installed base of 3D printers globally [1]. In FFF, an object is built by depositing melted material in a pre-determined path layer-by-layer. The materials used are thermoplastic polymers that come in a filament form.

The FFF process works by loading a 1.75- or 3-mm diameter spool of thermoplastic filament into the printer. Once the nozzle and print bed have reached their desired temperature, the filament is fed to the extrusion head and in the nozzle where it melts. The extrusion head is attached to a 3-axis system that allows it to move in the X, Y and Z directions. The melted material is extruded in thin strands and deposited layer-by-layer in predetermined locations, where it cools and solidifies. The cooling of the material is accelerated by a cooling fan attached to the extrusion head. To fill an area, multiple passes are required. When a layer is finished, the

build platform moves down, and a new layer is deposited. This process is repeated until the part is complete.

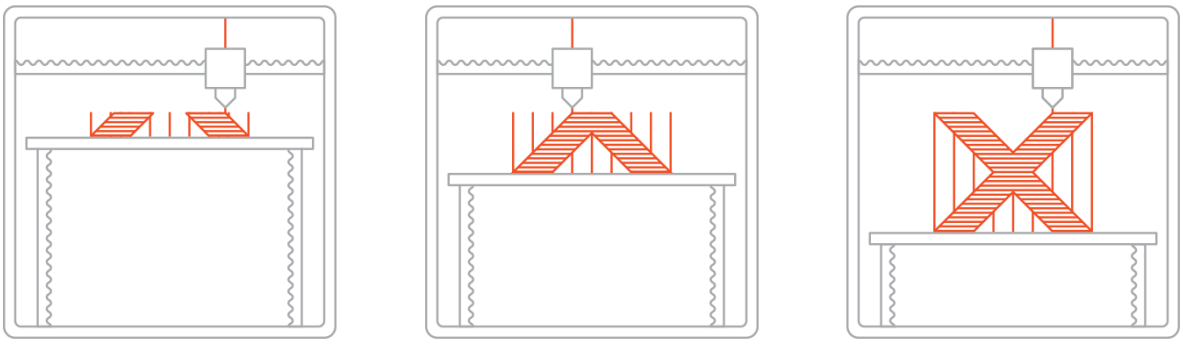

Figure 1: The FFF printing process [1].

One of the key strengths of FFF is the extensive range of available materials. These materials can be commodity thermoplastics (such as PLA and ABS), engineering materials (such as PA, TPU, and PETG), or high-performance thermoplastics (such as PEEK and PEI). The material used will affect the mechanical properties and accuracy of the printed part, along with its price.

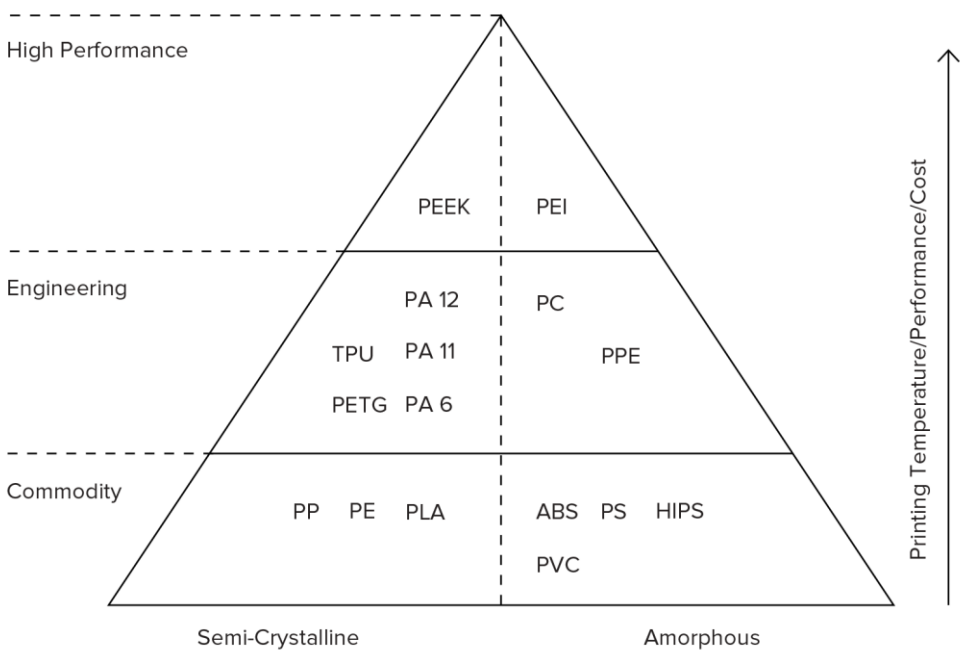

Figure 2: Thermoplastic materials pyramid available in FFF [1].

Polylactic acid (PLA) filament is the most popular material used in FFF 3D printing. It is an eco-friendly, biodegradable 3D printing material, made from annually renewable resources, corn starch or sugarcane, and requires less energy to process than traditional petroleum-based plastics. PLA filament is easy to use and aesthetically pleasing material, coming in many colors and additives, making it ideal for a wide range of applications.

PLA is the most extensively researched and utilized biodegradable aliphatic polyester in human history. Commonly made from alpha hydroxy acids, which include glycolic acid, lactic acid, citric acid, and mandelic acid, PLA is considered biodegradable and compostable.

PLA is a thermoplastic, high-strength, high-modulus polymer that can be made from annually renewable resources. The term thermoplastic defines the processability of a material as the temperature is changed. “A polymer that becomes plastic and flows on heating, by crystal melting or by exceeding the glass-transition temperature, T_G, is thermoplastic. This process is

reversible, and the material can be processed by extrusion after it has been prepared as a solid" [8]. PLA homopolymers have a glass-transition and melt temperature of about 55 °C and 175 °C, respectively. They require processing temperatures more than 185 ° – 190 °C. Crystalline PLA is soluble in chlorinated solvents and benzene at elevated temperatures. The mechanical properties and crystallization behavior of PLA is extremely dependent on the molecular weight and stereochemical makeup of the backbone [9].

Pure PLA has difficulty meeting all the requirements that a specific field may demand. As a result, PLA based composites have been extensively investigated over the past few decades. PLA based composites include PLA based copolymers in nanometer size and nanocomposites with PLA or PLA copolymers as matrix and nanofillers as the binding agent. The small-scale effect and surface effect of nanomaterials help improve the properties of PLA and make PLA based nanocomposites more popular compared with pure PLA materials.

Metallic nanoparticles are considered the most promising because they contain remarkable antibacterial properties due to their large surface area to volume ratio [22]. Among all the noble metal nanoparticles, silver nanoparticles have gained interest because of their unique properties such as chemical stability, good conductivity, catalytic and most important antibacterial activities. The metal releases silver ions, which have a strong cytotoxic effect on fungi, protozoa, several viruses, and both gram-positive and gram-negative bacteria [2,3,4].

In silver microstructure synthesis, Ethylene Glycol (EG), polyvinylpyrrolidone (PVP), and silver nitrate ($AgNO_3$) function as the polyol, capping agent, and salt precursor, respectively [Wiley et al., 2005]. The process proceeds by the chemical reduction of silver ion in the presence of a polymeric capping agent. A small amount of appropriate salt can further facilitate the growth of the silver seeds to the desired shape. The EG acts as both solvent and reducing agent

[Hemmati et al., 2015]. EG is converted to Glycol Aldehyde (GA), which is the reducing agent for silver ions according to the following equation [Hemmati et al., 2015].

$$2HOCH_2CH_2OH + O_2 \xrightarrow{160\ ^\circ C} 2HOCH_2CH_2O + H_2O$$

Due to the presence of the capping agent, which can be chemically attached to the surface of the silver seed by oxygen-silver bonding, the silver seeds are thoroughly distributed in the reaction solution. The attachment of the PVP to the silver seeds is shown in the following equation [Hemmati et al., 2015]. Purging with nitrogen gas provides an anoxic atmosphere and the wires can grow into shape.

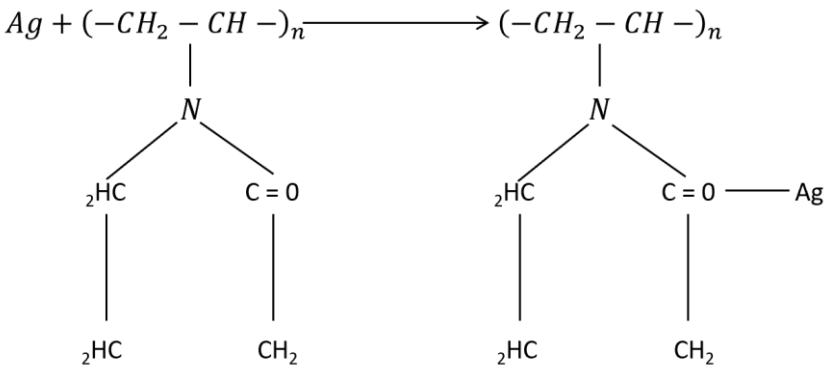

This thesis investigates the use of silver as an additive in PLA filaments for use with commercially available FFF systems. A wide variety of micro- and nanoscale additives have been previously explored as a means of modifying the properties of, or adding additional functionality to, thermoplastics. This thesis examines the use of silver microparticles and high aspect ratio silver wires with diameters in the micrometer range in an effect to reduce the challenges related to processability and toxicity that may exist from nanoparticle additives while still maintaining favorable surface interactions with the polymer matrix [5,6,7]. Silver microparticles in PLA composite filaments were explored as a precursor preliminary study. The

use of silver submicron wire in PLA composite filaments for FFF printing of antibacterial objects is assessed and the impact on the mechanical behavior of the material is investigated.

III. Experimental

A. Materials

PLA polymer pellets (NatureWorks, 3D850) were purchased from Filabot (Barre, VT). Silver powder (APS 1 – 3 µm, 99.9% metal basis) was purchased from Alfa Aesar by Thermo Fisher Scientific. Polyvinylpyrrolidone (PVP) powder (average M_w ~55,000), silver nitrate (99.9999% trace metal basis) and anhydrous ethylene glycol (99.8%) were purchased from Sigma-Aldrich. Toluene (reagent, ACS, 99.5%), chloroform (approximately 0.75% Ethanol as Preservative/HPLC), phosphate buffered saline (PBS) and BD Bacto tryptic soy broth were purchased from Fischer Scientific. Tryptic Soy Agar (TSA) CRITERION was purchased from Hardy Diagnostics. *Escherichia coli* (85W1660) was purchased from Ward Science.

B. Synthesis and Material Processing

1. Silver Submicron Wires Synthesis

Silver Submicron Wires (Ag SMWs) with PVP coatings were produced in this thesis using the polyol synthesis method [Wiley et al., 2005; Sun and Xia, 2002]. Ethylene glycol (50 mL) was heated to 60°C in a reaction flask and degassed under vacuum for four hours using a Schlenk line. Two separate solutions of silver nitrate and PVP were prepared in 30 mL of ethylene glycol. These solutions were simultaneously injected with a syringe pump into the reaction flask heated to 160°C under a nitrogen atmosphere at a rate of 375 mL per minute. The product was washed with toluene and collected by centrifugation at 5,000 rpms for 15 minutes. The molar ratio of silver nitrate to PVP was prepared at 1.5 and the concentration of silver nitrate to the total ethylene glycol volume was 0.085M.

2. Silver Microparticle Composite Granule Production

2. Silver Microparticle (Ag MP)-PLA composite granules were prepared as feedstock for extrusion of FFF filaments for 3D printing test specimens. PLA pellets were added to chloroform and stirred vigorously at 50 °C until they were dissolved forming a 100 g/L solution. Ag MPs with PVP were then added drop-wise from a separate chloroform solution and stirred for two hours. The solution was removed from heat and allowed to dry under ambient conditions for 48 hours. Residual solvent was removed from the dried composite in a vacuum oven at 50 °C for 24 hours. The composite was mechanically ground in a Dynisco Minigran granulator and passed through a 5-mm screen. The granulated composite was dried for an additional 24 hours under vacuum at 50 °C before use.

3. Silver Submicron Wires Composite Granule Production

Ag SMW-PLA composite granules were prepared as feedstock for extrusion of FFF filaments for 3D printing test specimens. PLA pellets were added to chloroform and stirred vigorously at 50°C until they were dissolved forming a 100 g/L solution. Ag SMWs were then added drop-wise from a separate chloroform solution and stirred for two hours. The solution was removed from heat and allowed to dry under ambient conditions for 48 hours. Residual solvent was removed from the dried composite in a vacuum oven at 50°C for 24 hours. The composite was mechanically ground in a Dynisco Minigran granulator and passed through a 5-mm screen. The granulated composite was dried for an additional 24 hours under vacuum at 50°C before use.

4. Filament Extrusion

Ag MP-PLA composite filaments and Ag SMW-PLA composite filaments were extruded using a single screw Filabot EX2 filament extruder. The composite granules were added to the

system hopper and extruded at 180°C at a rate of approximately 120-180 cm per minute. The composite was extruded through a 1.75 mm die. PLA filaments without Ag MP and Ag SMW additives were prepared with granules produced using the same procedures described in Section III.B.2 and III.B.3 to exclude any variation of antibacterial or mechanical testing results associated with the composite granule processing method.

5. Fused Filament Fabrication of Test Specimen

All specimens were printed on a Fusion3 F400-S FFF system. A custom printing profile was used to control the slicing/printing software which allowed printing in a single specified raster orientation for the entire specimen. Each specimen was printed individually at the center of the printing bed to reduce variations because of print bed location. For all specimens, two shells were used on the perimeter of the specimen and the inside of the specimen was printed with 100 percent infill. The raster direction was aligned along the long axis of the tensile test specimens to maximize the mechanical strength [Dul et al., 2016; Wu et al., 2015; Yang et al., 2017; Perez et al., 2014]. The specimens were printed with a nozzle temperature of 215°C at a speed of 4,100 mm/min and a print bed temperature of 60°C. Figure 3 shows the raster orientation tested and its definition.

C. Material Characterization

1. Electron Microscopy

A scanning electron microscope (SEM) scans a focused electron beam over a surface to create an image. The electrons in the beam interact with the sample, producing various signals that can be used to obtain information about the surface topography and composition. SEM images provide information about length, diameter, morphology, density, spatial distribution,

and structural arrangement. Morphology and fracture surfaces of tensile test specimens were observed using a Hitachi S-4800 SEM at an accelerating voltage of 3 keV. Fracture surfaces were sputter-coated with a 10 nm thick conductive gold film before imaging.

2. Differential Scanning Calorimetry

Knowledge of the thermal properties of polymers is vital for developing processing methods. Differential scanning calorimetry (DSC) is an effective analytical tool for characterizing physical properties. DSC enables the determination of the melting, crystallization, and mesomorphic transition temperatures along with the characterization of the glass transition and other effects which show either changes in heat capacity or latent heat [12]. Because of its simplicity and ease of use DSC is widely applied in polymer science [12]. Figure 3 shows the graphical results of a typical DSC scan.

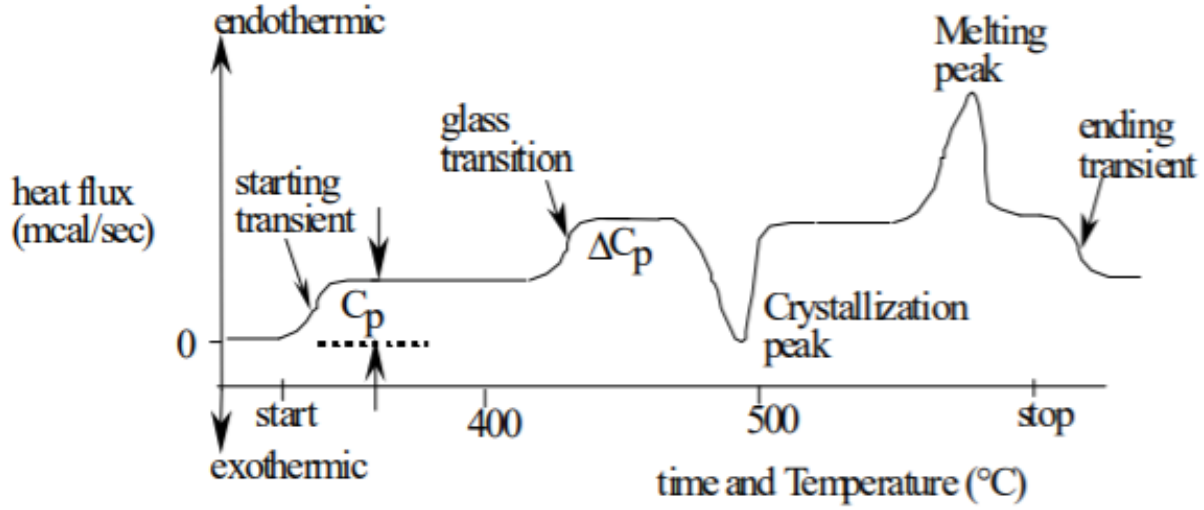

Figure 3: Typical DSC scan.

DSC was performed on a TA Instruments SDT Q600 TGA-DSC in an argon atmosphere. Samples were heated from 25°C to 250°C at a rate of 10°C/min. A single scan was performed to

obtain the glass transition temperature (T_G) and melting point (T_M) as a guide for FFF printer extrusion and print bed temperature set points.

3. Tensile Testing

FFF-printed tensile test specimens were tested based on the ASTM D638 standard test methods for tensile properties of plastics. The specimens were printed using the Type V specifications stated in the standard (see figure 4). It should be noted that the FFF process imparts an anisotropy in the specimen microstructure because of the stacking of deposited filaments that is not present in the standard. Each specimen was individually measured (thickness and width) at several locations throughout the test section. According to the ASTMs, the smallest cross-sectional area was used to determine the appropriate stress values.

Specimen were tested according to ASTM D638 Standard Test Methods for Tensile Properties of Plastics [13]. Tensile testing of the specimens was conducted at room temperature (approximately 20°C) on a MTI Instruments SEMtester 2000 with a 9 kN load cell. Stress was applied at a rate of 6 mm/min with data collected at 10 Hz. Six specimens were tested at each of the concentrations in this thesis.

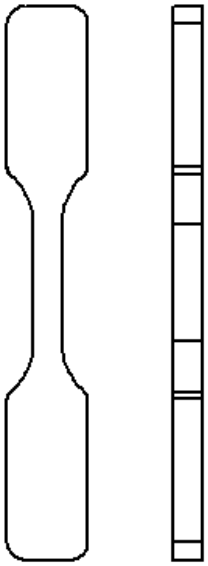

Figure 4: Tensile test design specimen.

4. Antibacterial Testing

The antibacterial activities of test specimens were obtained against *E.coli* strain 85W1660. *E.coli* was cultured in TSB at 37°C for 18 – 24 hours. The cultured bacteria were added to a 4 mL 0.9 percent saline solution to reach approximately the concentration of 10^8 CFU/mL. A portion of the saline solution containing the bacteria was diluted to 10^6 CFU/mL. Three 2.5 cm diameter dishes (see figure 5) were printed for 0.1 and 1.0 weight percent concentration level of Ag MP-PLA composites and 0.1, 1.0, and 10.0 weight percent concentration level of Ag SMW-PLA composites. Processed PLA with no additive was used as a control. The printed dishes were placed in sterilized petri dishes and 500 mL of the saline solution with the cultured bacteria was added drop-wise. The samples were covered and left at room temperature for 24 hours. After 24 hours, the bacteria containing drops were washed from the surface of the printed dishes using 1 mL of PBS. Then, 100 mL each of the bacteria suspension was dispersed onto TSA culture

medium. After incubation for 24 hours at 37°C, the surface area coverage of bacteria on the culture medium were measured using imageJ image processing software.

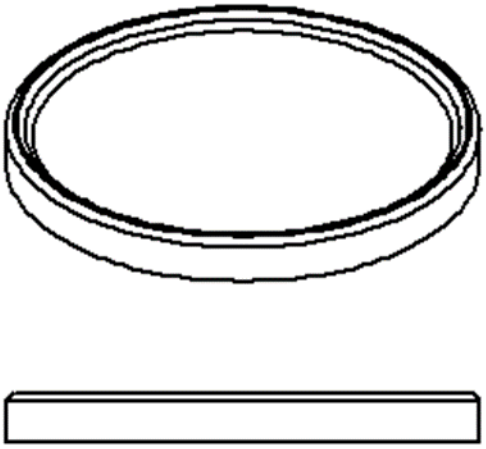

Figure 5: Antibacterial test design specimen.

IV. Results and Discussion

A. Silver Microparticle Morphology, Composite Processing, and Thermal Properties

SEM micrographs (Figures 6 and 7) of the Ag MPs produced in this thesis display two separated singular silver microparticles after sonication with PVP in chloroform and the silver microparticles natural tendency to agglomerate, respectively. The microparticles had an average particle size of 1 – 3 µm.

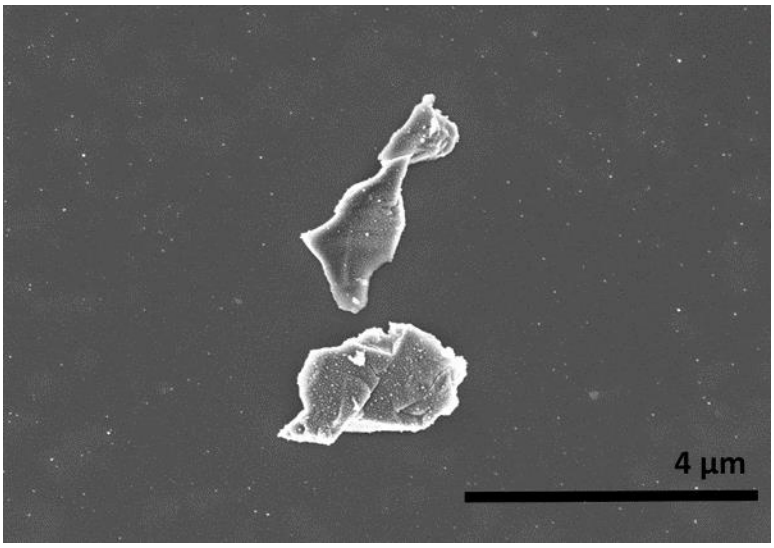

Figure 6: SEM micrograph of polyvinylpyrrolidone silver microparticles produced in this thesis [4 µm].

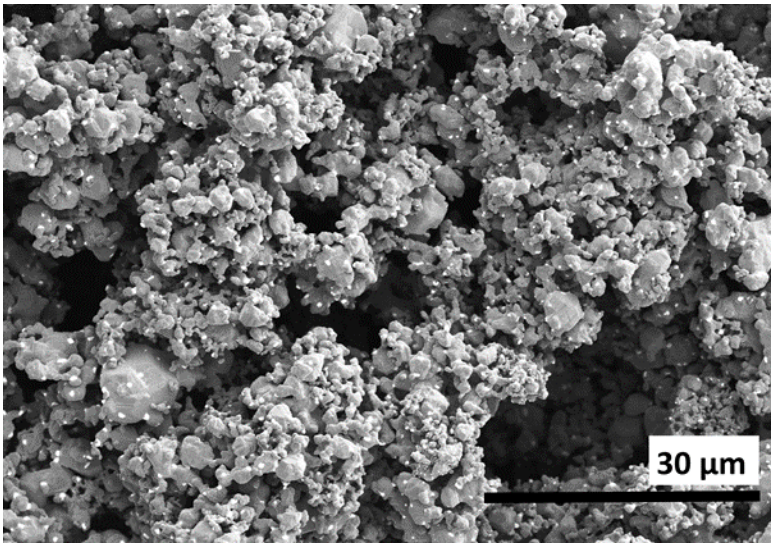

Figure 7: SEM micrograph of polyvinylpyrrolidone silver microparticles produced in this thesis [30 µm].

DSC curves of the Ag MP composites are shown in Figure 8 compared to PLA containing no additives. The data indicate that the composite filaments produced have glass transition temperatures (T_G) and melting points (T_M) that do not vary significantly from the plain PLA filaments. Specific values extracted from the DSC curves are indicated in Table 1. The results indicate that no change is required for FFF process parameters for the composites.

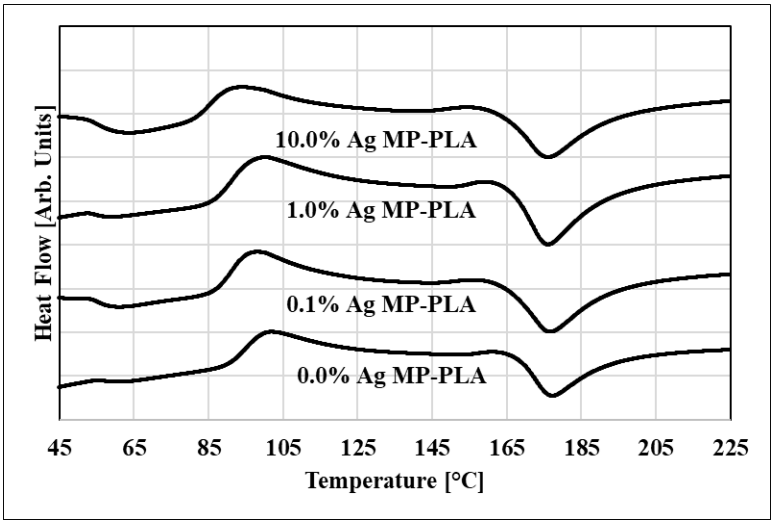

Figure 8: DSC data for 0.0, 0.1, 1.0 and 10.0 weight percent silver microparticle additives in polylactic acid.

Table 1: Glass transition temperatures (T_G) and melting points (T_M) extracted from DSC data.

Filament	T_G [°C]	T_M [°C]
PLA	57.3	177.4
0.1% Ag MP-PLA	55.6	176.8
1.0% Ag MP-PLA	55.7	176.2
10.0% Ag MP-PLA	55.7	176.2

B. Silver Microparticle Tensile Testing

The ultimate tensile strength of the FFF-printed test specimens decreased moderately with increasing Ag MP concentration, while the elastic modulus did not change significantly (Figures 9 and 10). The ductility of the test specimens, indicated by the strain at fracture displayed in Figure 11, declines at the highest Ag MP concentration. The ductility of solvent-processed PLA composites has been observed to increase in other studies because of residual solvent acting as a plasticizer at relatively low additive concentrations, which changes to brittle behavior at higher concentrations where the additive becomes dominant [Blattmann et al.,2016; Fortunati et al.,2012a, 2012b; Rhim et al., 2006]. The lack of increased ductility indicated in this thesis suggests that the repeated drying steps described in Section III.B.2 sufficiently removes any residual solvent present in the composite mixture. Therefore, the decreased ductility is likely a result of agglomeration or an increase in defect density because of poor additive-polymer interfacial interactions at high additive concentrations. Poor interfacial adhesion would also explain the observed trend of decreasing ultimate tensile strength with increasing Ag MP concentration and the lack of any significant change displayed by the elastic modulus.

Table 2: Summary of silver microparticle tensile testing results.

Filament	Ultimate Strength [GPa]	Strain at Fracture [%]	Modulus of Elasticity [GPa]
PLA	0.0574	0.0212	3.109
0.1% Ag MP-PLA	0.0521	0.0197	3.301
1.0% Ag MP-PLA	0.0438	0.0190	2.743
10.0% Ag MP-PLA	0.0423	0.0177	3.217

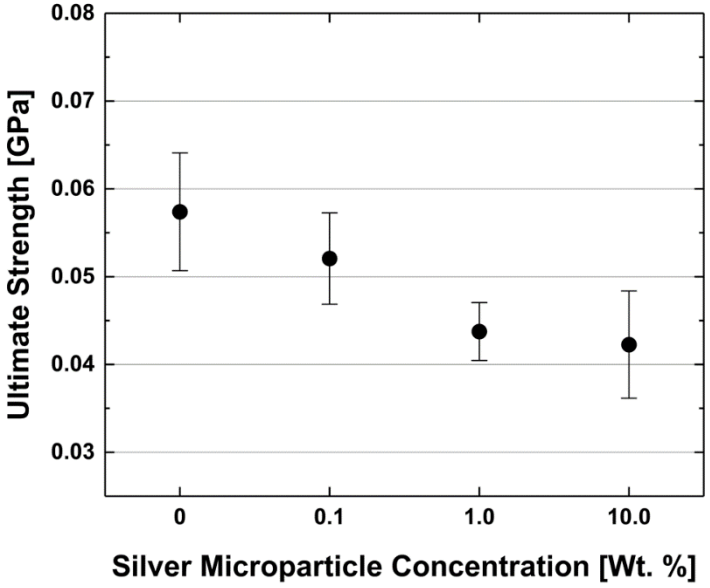

Figure 9: Ultimate strength versus silver microparticle concentration for fused filament fabrication printed tensile test specimen.

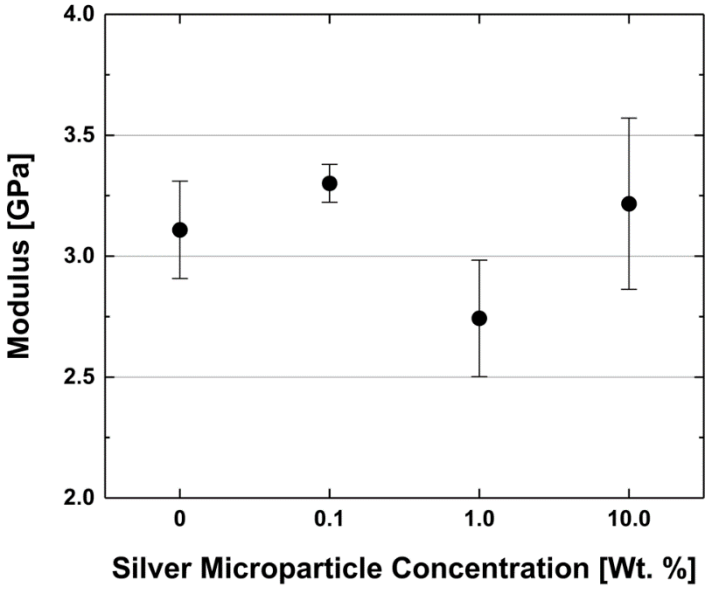

Figure 10: Modulus versus silver microparticle concentration for fused filament fabrication printed tensile test specimen.

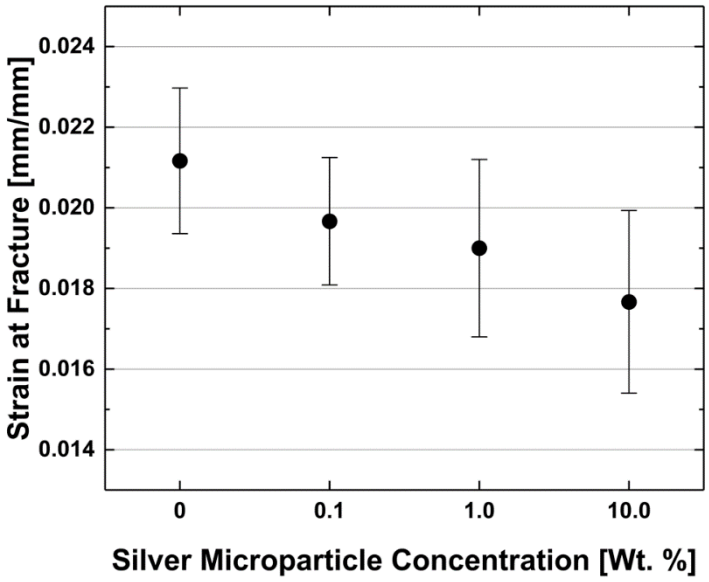

Figure 11: Strain at fracture versus silver microparticle concentration for fused filament fabrication printed tensile test specimen.

C. Silver Submicron Wire Morphology, Composite Processing, and Thermal Properties

The molar ratio between PVP and $AgNO_3$ in the polyol synthesis controls the morphology of the silver particles [Wiley et al., 2005; Sun and Xia, 2002]. SEM micrographs (Figures 12 and 13) of the Ag SMWs synthesized in this thesis display the characteristic faceted cross-section that results from anisotropic growth from dodecahedral seed particles containing multiple twin defects that are prevalent with low precursor concentrations [Wiley et al., 2005]. The wires had an average diameter of 0.330 mm ± 0.170 mm with an average aspect ratio larger than 20 and a range of 0.98 μm to 24.17 μm in length.

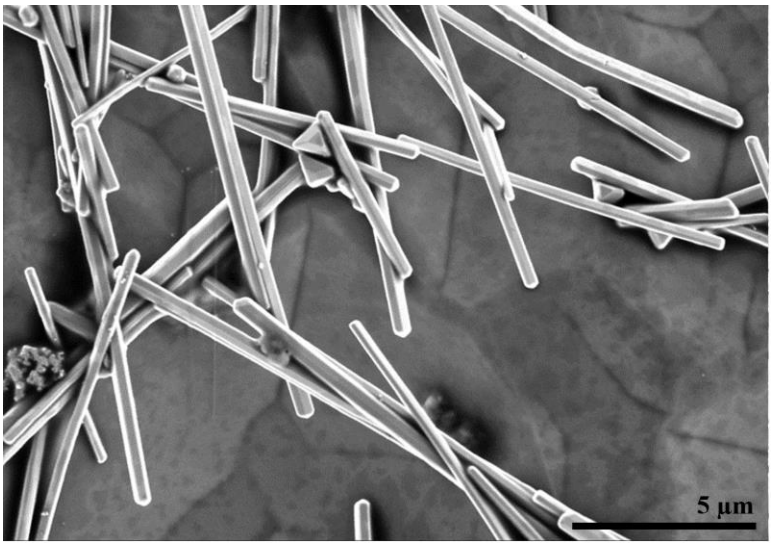

Figure 12: SEM micrograph of polyvinylpyrrolidone silver submicron wires synthesized in this thesis [5 μm].

Figure 13: SEM micrograph of polyvinylpyrrolidone silver submicron wires synthesized in this thesis [10 µm].

DSC curves of the Ag SMW composites are shown in Figure 14 compared to PLA containing no additives. The data indicate that the composite filaments produced have glass transition temperatures (T_G) and melting points (T_M) that do not vary significantly from the plain PLA filaments. Specific values extracted from the DSC curves are indicated in Table 2. This is consistent with observations of Ag nanowire-polymer composites in studies by Doganay et al. and Damm et al. The results indicate that no change is required for FFF process parameters for the composites studied herein.

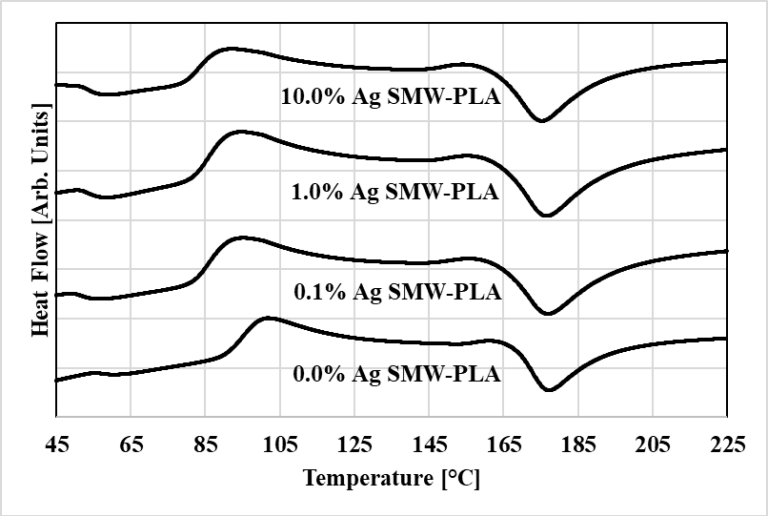

Figure 14: DSC data for 0.0, 0.1, 1.0 and 10.0 weight percent silver submicron wire additives in polylactic acid.

Table 3: Glass transition temperatures (T_G) and melting points (T_M) extracted from DSC data.

Filament	T_G [°C]	T_M [°C]
PLA	57.3	177.4
0.1% Ag SMW-PLA	52.0	177.0
1.0% Ag SMW-PLA	53.8	176.7
10.0% Ag SMW-PLA	53.8	175.4

D. Silver Submicron Wire Tensile Testing and Fractography

The ultimate tensile strength of the FFF-printed test specimens decreased moderately with increasing Ag SMW concentration, while the elastic modulus did not change significantly (Figures 15 and 16). The ductility of the test specimens, indicated by the strain at fracture displayed in Figure 17, declines at the highest Ag SMW concentration. The ductility of solvent-processed PLA composites has been observed to increase in other studies because of residual solvent acting as a plasticizer at relatively low additive concentrations, which changes to brittle behavior at higher concentrations where the additive becomes dominant [Blattmann et al.,2016;

Fortunati et al.,2012a, 2012b; Rhim et al., 2006]. The lack of increased ductility indicated in this thesis suggests that the repeated drying steps described in Section IV.B.3 sufficiently removes any residual solvent present in the composite mixture. Therefore, the decreased ductility is likely a result of agglomeration or an increase in defect density because of poor additive-polymer interfacial interactions at high additive concentrations. The PVP coating on the Ag SMWs allows for good dispersibility in the chloroform solution, but no significant interaction is expected between the PVP coating and PLA. Poor interfacial adhesion would also explain the observed trend of decreasing ultimate tensile strength with increasing Ag SMW concentration and the lack of any significant change displayed by the elastic modulus.

Table 4: Summary of silver submicron wire tensile testing results.

Filament	Ultimate Strength [GPa]	Strain at Fracture [%]	Modulus of Elasticity [GPa]
PLA	0.0574	0.0212	3.109
0.1% Ag SMW-PLA	0.0526	0.0188	3.367
1.0% Ag SMW-PLA	0.0487	0.0193	3.081
10.0% Ag SMW-PLA	0.0468	0.0165	3.335

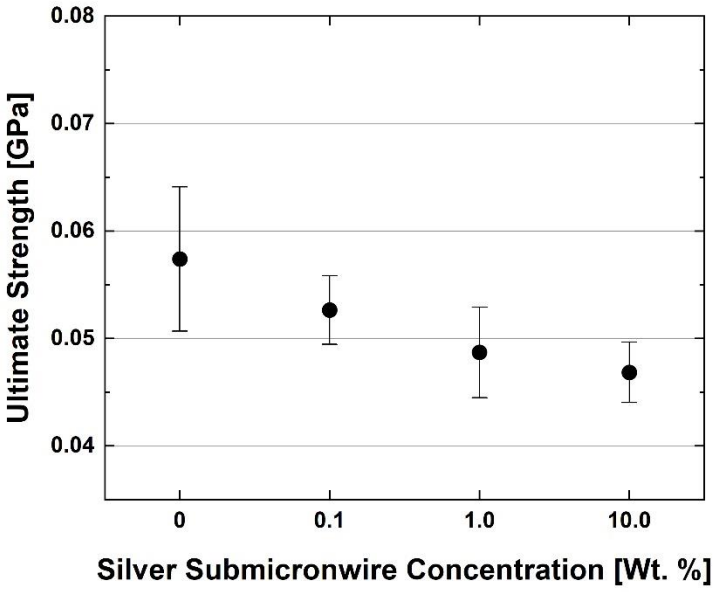

Figure 15: Ultimate strength versus silver submicron wire concentration for fused filament fabrication printed tensile test specimen.

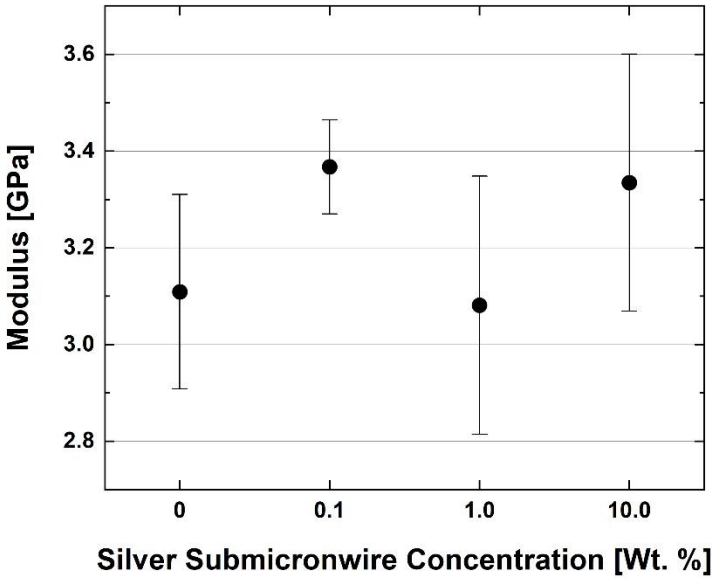

Figure 16: Modulus versus silver submicron wire concentration for fused filament fabrication printed tensile test specimen.

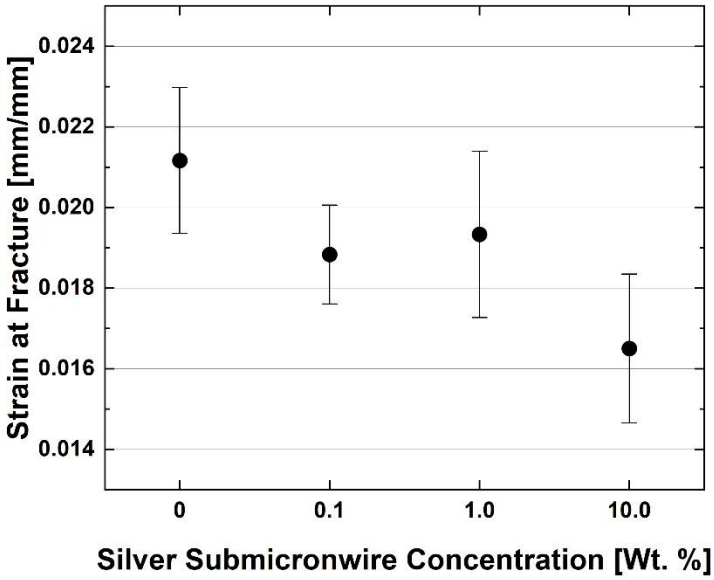

Figure 17: Strain at fracture versus silver submicron wire concentration for fused filament fabrication printed tensile test specimen.

SEM images of the fracture surfaces of FFF-printed test specimens fractured under tensile load provide further insight into the mechanical behavior observed. Figure 5 shows the presence of flat planes indicative of brittle fracture commonly observed for semi-crystalline polymers [Kinloch and Young, 1995]. The fracture surfaces also show Ag SMWs largely aligned perpendicular to the surface (Figure 6) indicating preferential alignment because of shear forces present in the extrusion head of the printing system. Void defects are also observed between the Ag SMWs and the PLA matrix throughout the specimens, indicative of poor bonding between the additive and polymer matrix. This is further indicated by the presence of wires jutting out above the fracture surface (Figure 6) denoting pull-out behavior associated with the lack of significant interfacial bonding. No obvious agglomeration of additives was observed on fracture surfaces; therefore, the addition of the large density of void defects within the specimen is the likely reason for the reduced strength and ductility.

The specimen cross-sections display a microstructure with interstitial voids between the deposited filaments and stacked layers that is the characteristic of FFF-printed objects [Gibsonet al., 2015]. A reduction of interstitial void size can be observed in the representative fracture surfaces in Figure 5 as the additive concentration increases. The shape of deposited beads and resulting void size in the FFF process is a result of several factors including the viscosity of the melted material, the print surface and interactions between the print nozzle and the bead [Gibson et al., 2015; Khaliq et al., 2017; Costa et al., 2018]. Notably, Costa et al. showed that a reduced viscosity led to greater coalescence and adhesion between extruded filaments. The presence of nanoparticles in a polymer matrix can dramatically reduce the viscosity of a composite [Kalathi

et al., 2012]. Therefore, it is likely that the viscosity of the melt is reduced with increasing Ag SMW additive concentration, but the details of this phenomenon are left to future studies. Despite the greater infill observed at higher additive concentrations, the ultimate strength and ductility are still reduced indicating that the increased contact area between deposited filaments does not play a dominant role in determining the mechanical behavior analyzed in this thesis.

E. Antibacterial Testing

The results of the antibacterial testing against *E.coli* are shown in Figures 7 and 8. The antibacterial effect of 0.1 and 1.0 weight percent silver microparticle composite printed specimen were tested. The results of the antibacterial testing against *E. coli* are shown in Table 18 and Figure 43. A reduction in bacteria growth is observed for 0.1 and 1.0 weight percent concentrations.

Table 5: *E. coli* growth versus silver microparticle concentration.

Filament	Bacteria Growth [%]	Reduction in Bacteria Growth [%]
PLA	94.1	-
0.1% Ag MP-PLA	87.7	6.4
1.0% Ag MP-PLA	80.3	13.8

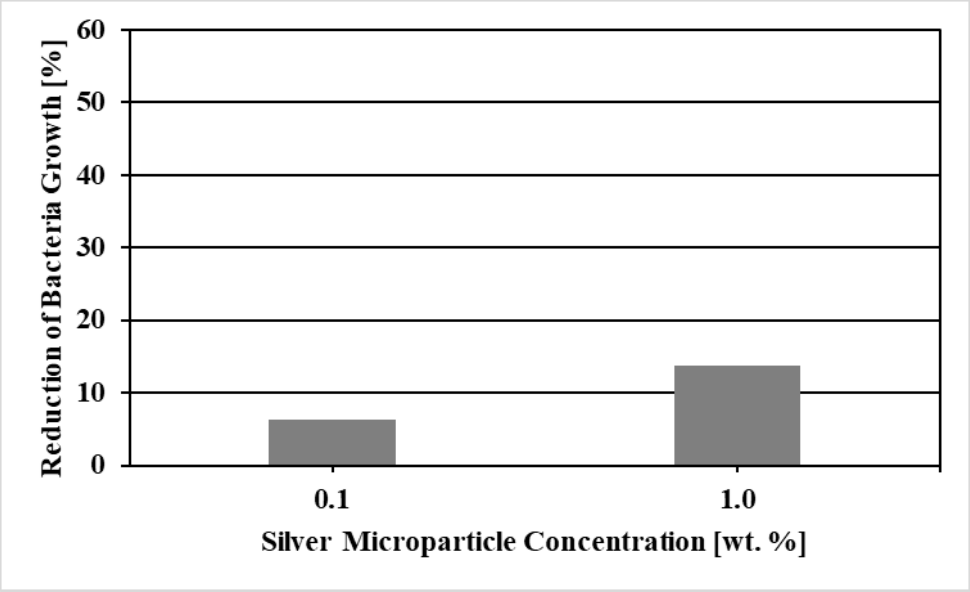

Figure 18: Reduction of *E. coli* growth versus silver microparticle concentration.

A negligible reduction in bacteria growth is observed for 0.1 and 1.0 weight percent silver submicron wire concentrations. However, significant antimicrobial activity is observed at the 10.0 weight percent silver submicron wire concentration with a reduction in growth close to 44 percent (table X). Silver ion release from the composite is the primary mechanism for the reduction of bacteria growth [LeOuay and Stellacci, 2015; Chernousova and Epple, 2015]. Bacteria likely make some direct contact with silver additives located on the surface of the composite, but ions are expected to reach the bacteria primarily through the diffusion of water into the bulk of the polymer matrix [Palza et al., 2015; Damm et al., 2008; Ton-That and Jungnickel, 1999; Cioffi et al., 2005]. Therefore, the choice of polymer matrix for antibacterial metal composites and its associated rate of water diffusion have a significant impact on the additive concentration required. Based on reported values of the water diffusion coefficient of PLA, it is expected that water would penetrate to a depth of approximately 300 mm over the 24-hour period that the *E. coli* containing droplets are in contact with the composite surface [Yew et

al., 2005]. While only a relatively shallow penetration of water into the bulk polymer is expected, the presence of void defects observed in the microstructure around the silver submicron wires may also facilitate ion release.

Table 6: *E. coli* growth versus silver submicron wire concentration.

Filament	Bacteria Growth [%]	Reduction in Bacteria Growth [%]
PLA	94.1	-
0.1% Ag SMW-PLA	86.3	7.8
1.0% Ag SMW-PLA	90.6	3.5
10.0% Ag SMW-PLA	50.2	43.9

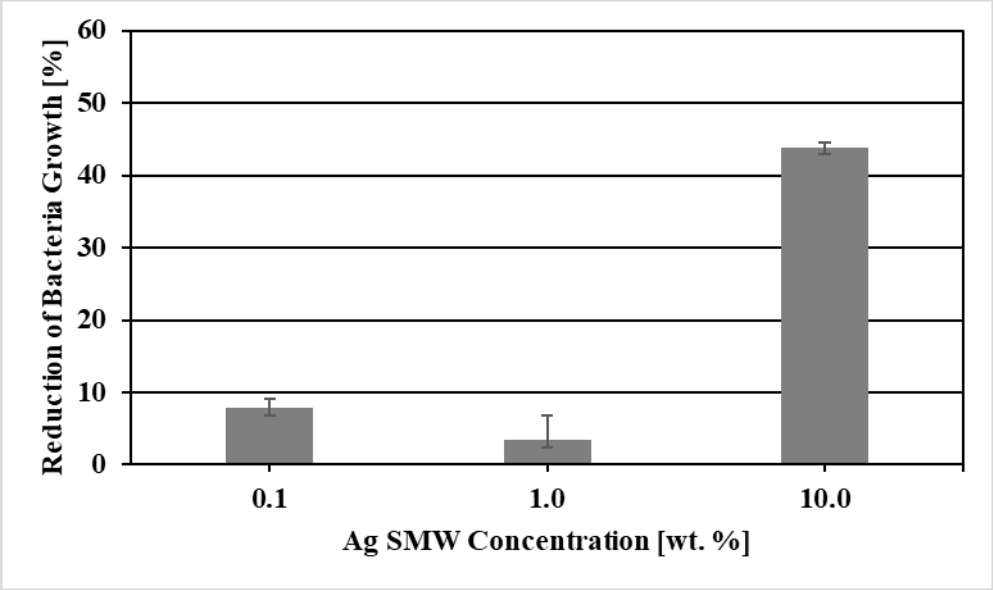

Figure 19: Reduction of *E. coli* growth versus silver submicron wire concentration.

V. Conclusions

Silver microparticles and submicron wires were assessed as an additive in PLA for applications in additive manufacturing. The silver microparticle and submicron wires additives were synthesized with a PVP coating and were processed with PLA to form composite granules using solvent processing and granulation. Composite granules with concentrations between 0.1 and 10.0 weight percent were used to extrude filaments that were compatible as feedstock for commercial FFF printing systems. The thermal properties of the composites studied in this thesis were relatively unchanged due to the silver microparticle and submicron wire incorporation allowing the printing of test specimens under identical printing process settings.

The impact of the addition of PVP-coated silver microparticle and submicron wires on the tensile mechanical properties was measured. The strain at fracture of FFF-printed test specimens was significantly reduced at the highest concentration of silver microparticles and submicron wires in PLA and the ultimate tensile strength declines systematically with increasing concentrations of silver microparticles and submicron wires. The modulus of elasticity did not change greatly, staying within a 95% confidence interval, for the concentrations studied. The reduced strength and ductility has been attributed to the increase in void defects observed between the silver submicron wire additives and the polymer matrix.

A strong antibacterial effect was observed against *E. coli* at the silver submicron wire additive concentration of 10.0 weight percent. The reduction of bacteria growth was attributed to the release of silver ions facilitated by the penetration of water into the bulk composite through diffusion and voids observed in the microstructure. The impact of the addition of PVP-coated silver submicron wires on the tensile mechanical properties was also considered. The strain at

break of FFF-printed test specimens was reduced at the highest concentration and the ultimate tensile strength declines systematically with increasing concentration.

The results demonstrate the efficacy of using silver microparticles and submicron wires in PLA composites for FFF-printing. Although a slight degradation of mechanical properties is observed as a result of incorporation of the additive compared to PLA, the composites have potential for a variety of applications. As a proof-of-concept, prototype surgical tools were printed using the silver submicron wires – PLA composite filaments (Figures 44 and 45). To reduce the degradation of the mechanical behavior, future work will explore additive coatings for improving interfacial adhesion with the polymer matrix for improving the mechanical behavior.

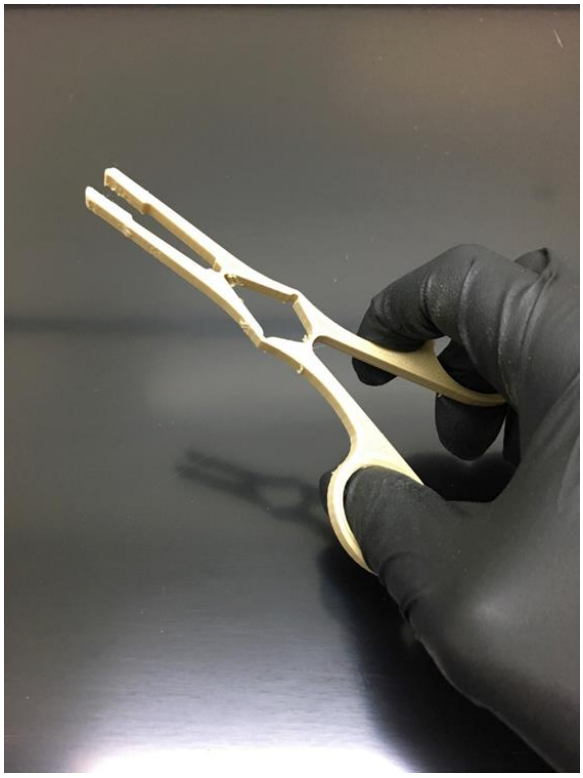

Figure 20: Surgical forceps 3D printed with Ag SMWs – PLA filament.

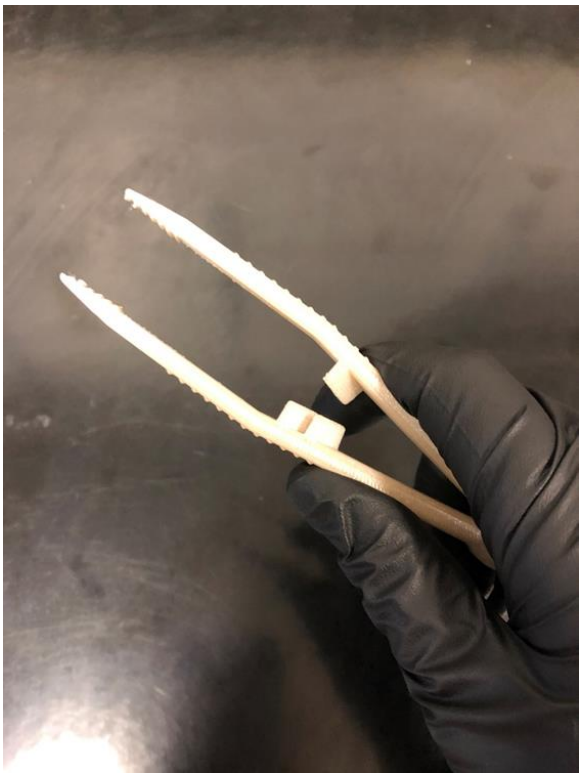

Figure 21: Surgical tweezers 3D printed with Ag SMWs – PLA filament.

References

Blattmann, C.O. and Pratsinis, S.E. (2016), "Nanoparticle filler content and shape in polymer nanocomposites", *Kona Powder and Particle Journal*, Vol. 36 No. 1, pp. 1-30.

Centers for Disease Control and Prevention (2017), "Current HAI progress report", available at: www.cdc.gov/hai/data/portal/progress-report.html (accessed 30 March 2019).

Chernousova, S. and Epple, M. (2015), "Silver as antibacterial agent: ion, nanoparticle, and metal", *Angewandte Chemie (International ed. In English)*, Vol. 52 No. 6, pp. 1636-1653.

Cioffi, N., Torsi, L., Ditarantano, N., Tantalillo, G., Ghibelli, L., Sabbatini, L., Bleve-Zacheo, T., D'Alessio, M., Zambonin, P.G. and Traversa, E. (2005), "Copper nanoparticle/polymer composites with antifungal and bacteriostatic properties", *Chemistry of Materials*, Vol. 17 No. 21, pp. 5255-5262.

Cloutier, M., Mantovani, D. and Rosei, F. (2015), "Antibacterial coatings: challenges, perspectives, and opportunities", *Trends in Biotechnology*, Vol. 33 No. 11, pp. 637-652.

Costa, A.E., Ferreira da Silva, A. and Carneiro, O.S. (2018), "A study on extruded filament bonding in fused filament fabrication", *Rapid Prototyping Journal*, Vol. 25 No. 3, pp. 555-565.

Damm, C., Munstedt, H. and Rosch, A. (2008), "The antimicrobial efficacy of polyamide 6/Silver-Nano- and microcomposites", *Materials Chemistry and Physics*,Vol. 108 No. 1, pp. 61-66.

Doganay, D., Coskun, S., Kaynak, C. and Unalan, H.E. (2016), “Electrical, mechanical and thermal properties of aligned silver nanowire/polylactide nanocomposite films”, *Composites Part B: Engineering*, Vol. 99, pp. 288-296.

Dul, S., Fambri, L. and Pegoretti, A. (2016), “Fused deposition modeling with ABS-Graphene nanocomposites”, *Composites Part A: Applied Science and Manufacturing*, Vol. 85, pp. 181-191.

Fortunati, E., Armentano, I., Zhou, Q., Puglia, D., Terenzi, A., Berglund, L.A. and Kenny, J.M. (2012a), “Microstructure and nonisothermal cold crystallization of PLA composites based on silver nanoparticles and nanocrystalline cellulose”, *Polymer Degradation and Stability*, Vol. 97 No. 10, pp. 2027-2036.

Fortunati,E.,Armentano,I.,Zhou,Q.,Iannoni,A.,Saino, E., Visai, L., Berglund, L.A. and Kenny, J.M. (2012b), “Multifunctional bionanocomposite films of poly(lactic acid), cellulose nanocrystals and silver nanoparticles”, *Carbohydrate Polymers*, Vol. 87 No. 2, pp. 1596-1605.

Gibson, I., Rosen, D. and Stucker, B. (2015), *Additive Manufacturing Technologies*, Springer, New York, NY.

Hemmati, Shohreh, et al. "Synthesis and Characterization of Silver Nanowire Suspensions for Printable Conductive Media." ECS Journal of Solid State Science and Technology 4.4 (2015): P3075-P3079.

Hussain, S. M., Braydich-Stolle, L. K., Schrand, A. M., Murdock, R. C., Yu, K. O., Mattie, D. M., Schlager, J. J. and Terrones, M. (2009), “Toxicity evaluation for safe use of

nanomaterials: recent achievements and technical challenges", *Advanced Materials*, Vol. 21 No. 16, pp. 1549-1559.

Jin, Y.-A., Plott, J., Chen, R., Wensman, J. and Shih, A. (2015), "Additive manufacturing of custom orthoses and prostheses – a review", *Procedia* CIRP, Vol. 36, pp. 199-204.

Kalathi, J. T., Grest, G. S. and Kumar, S. K. (2012), "Universal viscosity behavior of polymer nanocomposites", *Physical Review Letters*, Vol. 109 No. 19, p. 198301.

Khaliq, M. H., Gomes, R., Fernandes, C., Nóbrega, J. M., Carneiro, O. S. and Férras, L. L. (2017), "On the use of high viscosity polymers in the fused filament fabrication process", *Rapid Prototyping Journal*, Vol. 23 No. 4, pp. 727-735.

Kinloch, A.J. and Young, R.J. (1995), *Fracture Behaviour of Polymers*, Springer, New York, NY.

LeOuay, B. and Stellacci, F. (2015), "Antibacterial activity of silver nanoparticles: a surface science insight", Nano Today, Vol. 10, pp. 339-354.

Malik, H.H., Darwood, A.R., Shaunak, S., Kulatilake, P., El-Hilly, A.A., Mulki, O. and Baskaradas, A. (2015), "Three-Dimensional printing in surgery: a review of current surgical applications", *Journal of Surgical Research*, Vol. 199 No. 2, pp. 512-522.

Müller, K., Bugnicourt, E., Latorre, M., Jorda, M., Sanz, Y. E., Lagaron, J. M., Miesbauer, O., Bianchin, A., Hankin, S., Bölz, U., Pérez, G., Jesdinszki, M., Lindner, M., Scheuerer, Z., Castelló. and Schmid, M. (2017), "Review on the processing and properties of polmer nanocomposites and nanocoatings and their applications in the packaging, automotive and solar energy fields", *Nanomaterials*, Vol. 7 No. 4, pp. 1-47.

Page, K., Wilson, M. and Parkin, I. P. (2009), "Antimicrobial surfaces and their potential in reducing the role of the inanimate environment in the incidence of Hospital-Acquired infections", *Journal of Materials Chemistry*, Vol. 23, pp. 3819-3831.

Palza, H., Quijada, R. and Delgado, K. (2015), "Antimicrobial polymer composites with copper micro- and nanoparticles: effect of particle size and polymer matrix", *Journal of Bioactive and Compatible Polymers*, Vol. 30 No. 4, pp. 1-15.

Perez, A. R. T., Roberson, D. A. and Wicker, R. B. (2014), "3D printing for continuous fiber reinforced thermoplastic composites: mechanism and performance", *Journal of Failure Analysis and Prevention*, Vol. 14, pp. 343-352.

Rhim, J. W., Mohanty, A. K., Singh, S. P. and Ng, P. K. W. (2006), "Effect of the processing methods on the performance of polylactide films: thermocompression versus solvent casting", *Journal of Applied Polymer Science*, Vol. 101 No. 6, pp. 3736-3742.

Saini, P., Arora, M. and Kumar, M.N.V.R. (2016), "Poly (lactic acid) blends in biomedical applications", *Advanced Drug Delivery Reviews*, Vol. 107, pp. 47-59.

Society of Manufacturing Engineers (SME) Annual Report (2018), "Medical additive manufacturing/3D printing", available at: www.sme.org (accessed 30 March 2019).

Sun, Y. and Xia, Y. (2002), "Shape-control synthesis of gold and silver nanoparticles", *Science*, Vol. 298 No. 5601, pp. 2176-2179.

Ton-That, T. M. and Jungnickel, B. J. (1999), "Water diffusion into transcrystalline layers on polypropylene", *Journal of Applied Polymer Science*, Vol. 74 No. 13, pp. 3275-3285.

Wiley, B., Sun, Y., Mayers, B. and Xia, Y. (2005), "Shape control of silver nanoparticles", *Chemistry (Weinheim an Der Bergstrasse, Germany),* Vol. 11 No. 2, pp. 454-463.

Wu, W., Geng, P., Li, G., Zhao, D., Zhang, H. and Zhao, J. (2015), "Influence of layer thickness and raster angle on the mechanical properties of 3D-printed PEEK and a comparative mechanical study between PEEK and ABS", *Materials,* Vol. 8 No. 9, pp. 5834-5846.

Yang, C., Tian, X., Liu, T., Cao, Y. and Li, D. (2017), "3D printing for continuous fiber reinforced thermoplastic composites: mechanism and performance", *Rapid Prototyping Journal,* Vol. 23 No. 1, pp. 209-215.

Yew, G.H., Yusof, A.M.M., Ishak, Z.A.M. and Ishiaku, U.S. (2005), "Water absorption and enzymatic degradation of poly(lactic acid)/rice starch composites", *Polymer Degradation and Stability,* Vol. 90 No. 3, pp. 488-500.

Appendices

Test Results

Table 7: Tensile results of PLA specimen.

Specimen [#]	Ultimate Strength [Gpa]	Strain At Fracture [%]	Modulus of Elasticity [GPa]
1	0.0545	0.021	2.936
2	0.0464	0.018	3.020
3	0.0586	0.021	3.163
4	0.0652	0.022	3.457
5	0.0591	0.022	3.116
6	0.0605	0.023	2.961

Table 8: Tensile results of 0.1 wt. % Ag MPs in PLA specimen.

Specimen [#]	Ultimate Strength [Gpa]	Strain At Fracture [%]	Modulus of Elasticity [GPa]
1	0.0496	0.0180	3.326
2	0.0519	0.0190	3.283
3	0.0585	0.0210	3.266
4	0.0525	0.0190	3.209
5	0.0442	0.0220	3.292
6	0.0557	0.0190	3.431

Table 9: Tensile results of 1.0 wt. % Ag MPs in PLA specimen.

Specimen [#]	Ultimate Strength [Gpa]	Strain At Fracture [%]	Modulus of Elasticity [GPa]
1	0.0420	0.0180	2.830
2	0.0459	0.0180	2.982
3	0.0425	0.0220	2.357
4	0.0462	0.0200	2.926
5	0.0470	0.0200	2.746
6	0.0389	0.0160	2.616

Table 10: Tensile results of 10.0 wt. % Ag MPs in PLA specimen.

Specimen [#]	Ultimate Strength [Gpa]	Strain At Fracture [%]	Modulus of Elasticity [GPa]
1	0.0450	0.0170	3.226
2	0.0477	0.0180	3.270
3	0.0448	0.0150	3.471
4	0.0411	0.0210	2.609
5	0.0312	0.0160	3.576
6	0.0438	0.0190	3.148

Table 11: Tensile results of 0.1 wt. % Ag SMWs in PLA specimen.

Specimen [#]	Ultimate Strength [Gpa]	Strain At Fracture [%]	Modulus of Elasticity [GPa]
1	0.0532	0.0180	3.537
2	0.0520	0.0190	3.287
3	0.0502	0.0180	3.359
4	0.0558	0.0190	3.392
5	0.0561	0.0210	3.340
6	0.0485	0.0180	3.289

Table 12: Tensile results of 1.0 wt. % Ag SMWs in PLA specimen.

Specimen [#]	Ultimate Strength [Gpa]	Strain At Fracture [%]	Modulus of Elasticity [GPa]
1	0.0523	0.0180	3.440
2	0.0475	0.0170	3.255
3	0.0416	0.0180	2.900
4	0.0518	0.0200	3.209
5	0.0479	0.0220	2.839
6	0.0511	0.0210	2.844

Table 13: Tensile results of 10.0 wt. % Ag SMWs in PLA specimen.

Specimen [#]	Ultimate Strength [Gpa]	Strain At Fracture [%]	Modulus of Elasticity [GPa]
1	0.0483	0.0180	3.219
2	0.0484	0.0150	3.582
3	0.0478	0.0190	2.917
4	0.0427	0.0150	3.274
5	0.0495	0.0170	3.446
6	0.0443	0.0150	3.570

Table 14: Antibacterial results of PLA specimen.

Specimen [#]	Pixels Covered [#]	Pixels Total [#]	Bacteria Growth [%]
1	1393753	1463344	95.2444
2	1478395	1534752	96.3289
3	2781765	3069081	90.6384

Table 15: Antibacterial results of 0.1 wt. % Ag MPs in PLA specimen.

Specimen [#]	Pixels Covered [#]	Pixels Total [#]	Bacteria Growth [%]
1	3071020	3529108	87.0197
2	3109010	3468160	89.6444
3	2645869	3064982	86.3258

Table 16: Antibacterial results of 1.0 wt. % Ag MPs in PLA specimen.

Specimen [#]	Pixels Covered [#]	Pixels Total [#]	Bacteria Growth [%]
1	1093455	1596484	68.4914
2	1260781	1535976	82.0834
3	2689138	2976976	90.3312

Table 17: Antibacterial results of 0.1 wt. % Ag SMWs in PLA specimen.

Specimen [#]	Pixels Covered [#]	Pixels Total [#]	Bacteria Growth [%]
1	1491816	1745969	85.4434

2	2498346	2921696	85.5101
3	2553668	2905404	87.8937

Table 18: Antibacterial results of 1.0 wt. % Ag SMWs in PLA specimen.

Specimen [#]	Pixels Covered [#]	Pixels Total [#]	Bacteria Growth [%]
1	5324789	5995876	88.8075
2	5301520	5611256	94.4801
3	3170389	3580029	88.5576

Table 19: Antibacterial results of 10.0 wt. % Ag SMWs in PLA specimen.

Specimen [#]	Pixels Covered [#]	Pixels Total [#]	Bacteria Growth [%]
1	1177507	2328928	50.5600
2	1419426	2866726	49.5138
3	1256029	2485344	50.5374

Vita

Jenna Walker Robichaux was born in Prince William, Virginia and raised in Stafford. Before attending the University of New Orleans, she attended Louisiana State University, Baton Rouge, Louisiana where she earned a Bachelor of Science in Petroleum Engineering in 2017.

While at the University of New Orleans, Jenna was initiated into Tau Beta Pi and served on several committees, including the American Society of Mechanical Engineers, the Society of Women Engineers, and the AMRI Graduate Student Committee. Jenna also presented posters at the Innovate UNO and the Annual AMRI Mardi Gras Review.

Currently, Jenna is a Project Engineer at CDI Engineering Solutions, LLC in Baton Rouge, Louisiana. She lives in Hammond, Louisiana with her husband, Cameron.